Progress In Electromagnetics Research, Vol. 122, 61–76, 2012

DUAL CIRCULAR POLARIZED STEERING ANTENNA FOR SATELLITE COMMUNICATIONS IN X BAND

G. Expósito-Domínguez [1, *], J. M. Fernández-González [1], P. Padilla [2], and M. Sierra-Castañer [1]

[1]Radiation Group, Signals, Systems and Radiocommunication Department, Universidad Politécnica de Madrid, Ciudad Universitaria, Madrid 28040, Spain

[2]Department of Signal Theory, Telematics and Communications, Universidad de Granada, Periodista Daniel Saucedo Aranda, Granada 18071, Spain

Abstract—In this work, a dual circular polarized steering antenna for satellite communications in X band is presented. The antenna consists of printed elements grouped in an array. This terminal works in a frequency band from 7.25 GHz up to 8.4 GHz (15% of bandwidth), where both bands, reception (RX) and transmission (TX) are included simultaneously and Left Handed Circular Polarization (LHCP) and Right Handed Circular Polarization (RHCP) are interchangeable. The antenna is compact, narrow bandwidth and reaches a gain of 16 dBi. It has the capability to steer in elevation to 45°, 75°, 105° and 135° electronically with a Butler matrix and 360° in azimuth with a motorized junction.

1. INTRODUCTION

The increasing use of broadband satellite systems to provide ubiquitous and high-capacity communications demand lightweight and low-profile steerable-beam antennas with a small footprint that can be integrated on vehicles, trains or aircrafts. Therefore, an increasing demand for mobile satellite terminals is emerging [1]. These terminals require antenna frontends capable to track one or more satellites (uni/bidirectional) and to provide enough bandwidth at the same time. X band satellites are widely available and can easily provide rich multimedia broadcasting as well as broadband communications

Received 5 October 2011, Accepted 8 November 2011, Scheduled 14 November 2011

* Corresponding author: Gonzalo Expósito-Domínguez (gexposito@gr.ssr.upm.es).

services at a competitive cost with respect to other satellite systems at lower frequencies. Although, X band antenna terminals are generally expensive and heavy, phased array technology can provide low-profile and reliable solutions at a reasonable price for mass production.

The antenna array concept arises due to the necessity of getting higher directivity. By changing the phase feeding of the array elements the radiation pattern can be steered in the desired direction [2] without moving the antenna physically. This kind of feeding can be done through active networks such as phase shifters [3] or microelectromechanical systems (MEMS). Those systems have high complexity but high flexibility and features. In [4] four elements array is fed by coplanar transmission lines (TL). Using MEMS, those TLs change their capacity and propagation velocity, therefore the radiating elements can be fed with the desired phase shift. In [5], a complex system of 156 radiating elements in Ku band is presented. This system is constructed in Low Temperature Co-Fired Ceramic (LTCC) technology, it has linear polarization, and it can be used only in reception. In [6], a complex beamforming example is shown. This system works in L band and has return losses around -10 dB. Another beam control option is passive networks [7, 8], which do not have so good features but are cheaper solutions. In [9] and [10] a system based in horn antennas and beamforming networks is shown. This antenna is capable of using several beams simultaneously. On the other hand, solutions based in Traveling Wave Antennas (TWA) [11, 12], allow to control the direction of the radiation pattern as a function of frequency for a narrow band.

The aim of this work is the development of an onboard satellite communication system in X band. This printed antenna has the following capabilities: broadband capacity (7.25–8.15 GHz) 15%, (in [13] the design reaches 10%, in [14] the design reaches 111.7%), dual circular polarization (RHCP and LHCP, interchangeable for TX and RX), good axial ratio (AR $<$ 3 dB) as in [15] but with capability of beam steering (90° elevation) by means of a passive Butler network. The main contributions in this article are directly related to the requirements of the onboard antenna for a demanding satellite communication system. In this way, the contributions of this work can be grouped into two main concerns: a) the design and prototyping of a complete onboard radiation system which fulfill hard radiation pattern, isolation and loss requirements, and b) each element in the antenna design must also fulfill specifications not only when working alone but also combined with the rest of the elements; for instance, the hybrid couplers must guarantee a good matching and a wide working band considering hard constraints in terms of available space. What is more,

Table 1. Antenna specifications.

Parameter	Value	Comments
Polarization RX	LHCP	Left Handed Circular Polarization*.
Polarization TX	RHCP	Right Handed Circular Polarization*.
Gain	16 dBi	For the broadside direction.
Maximum Dimensions	< 0.2 m	Equivalent diameter.
Antenna Efficiency	$> 60\%$	Including network losses.
Axial Ratio	< 3 dB	Circular polarization purity.
CP/XP	> 25 dB	Co-polar and Cross-polar Ratio.
S_{11}	< -15 dB	Reflection coefficient.
S_{21}	< -15 dB	Isolation between frequency bands.

*Both are interchangeable.

interconnection issues between the different constituting elements are also a valuable work and a key concern in this document, since some strategies are also proposed and adapted for these particular antenna requirements. Table 1 shows the design specifications for this antenna.

This paper is organized as follows: Section 2 is devoted to the design process of the antenna in three stages: 2.1 presents the design of the array, 2.2 explains the steering network features and 2.3 the calculations for the array factor. In Section 3 complete prototypes are shown and measured. Finally, in Section 4 the conclusions are drawn.

2. DESIGN AND SIMULATIONS

The complete design of the antenna has been divided into two main parts: the radiating element and the Butler network to obtain the steering direction. The radiating elements are microstrip patches meanwhile the Butler network is based in hybrid couplers.

2.1. Array Design

The radiation pattern requirements of the complete system require a precise beam control and an adequate array configuration. Thus, the antenna is configured as a 4×4 circular microstrip patches array. These elements are treated in two different ways:

- Rows: First, the radiating elements are grouped in rows, separated a distance between them of $0.85\lambda|_{7.25\,\mathrm{GHz}}$ in order to increase the effective area and consequently the gain. Those elements are fed by an uniform passive distribution network (Figure 1).

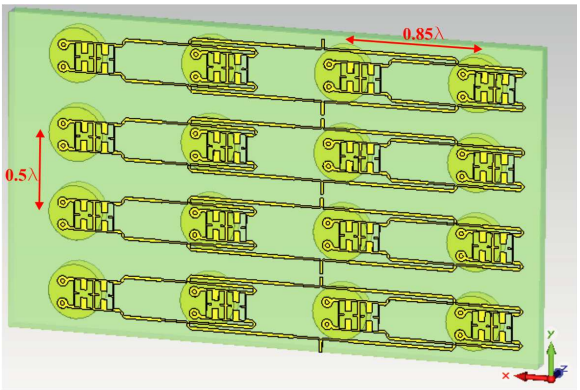

Figure 1. 4×4 array simulation model.

- Columns: Then, 4 rows of 4 elements are grouped vertically and separated $0.5\lambda|_{7.25\,\mathrm{GHz}}$, this separation avoids the gratings lobes effect. The steering direction of the main beam is achieved due to the phase shift between each row, given by the Butler network.

Each radiating element is composed of two stacked patches: the upper one is fed by electromagnetic coupling (thickness substrate $1 = 0.254\,\mathrm{mm}$), meanwhile the bottom one (thickness substrate $2 = 1.143\,\mathrm{mm}$) is fed by two via holes (diameter $= 1.1\,\mathrm{mm}$) to get the circular polarization, in [16] patches are fed by two slots, meanwhile in [17] patches are fed by L-probes. These vias are connected with a two-stages miniaturized hybrid coupler [18] which enhances the bandwidth of the circuit, permits two circular polarizations (RHCP and LHCP) at the same time, and increases the isolation between both channels (TX and RX). The two patches are separated by one foam layer (thickness $= 4\,\mathrm{mm}$) in order to get higher bandwidth (Figure 2) [19]. In the bottom part (thickness substrate $3 = 0.254\,\mathrm{mm}$), the feeding distribution network and connectors are placed. It is necessary to remark that specifications and space constraints make the network design a challenging one, since the hybrid couplers are especially shaped according to the available space. In order to introduce the distribution lines, and 1 to 4 dividers, the double stage hybrid couplers were miniaturized. This miniaturization reduces the dimensions from $10.90\,\mathrm{mm} \times 14.41\,\mathrm{mm}$ to $8.07\,\mathrm{mm} \times 10.67\,\mathrm{mm}$ (26%). Also the connection with the radiating array has to be carefully defined (in this case by means of via holes). The substrate permittivity is 2.17 in order to get good radiation of the antenna [20]. Despite the reduction of the Q factor, the substrates and foam thickness are high in order to enhance the bandwidth ($\sim 15\%$).

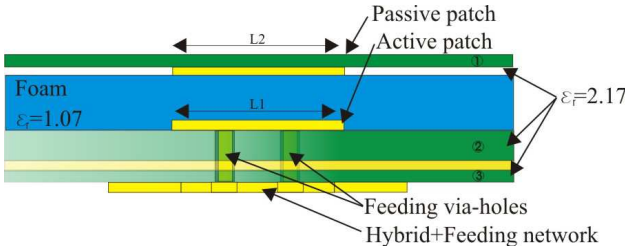

Figure 2. Radiating element layer view.

2.2. Butler Network

The Butler matrix is a passive network with 2^n inputs, 2^n outputs, $2^{n-1}\log_2 2^n$ hybrid couplers, crossovers and phase shifters [8]. The function of a Butler matrix is to combine signals in phase going to or coming from an antenna array. It produces 2^n beams with constant angular separation. Each output signal at n port (S_n) can be expressed as follows:

$$S_n = \sum_{m=1}^{n} A_m e^{j\alpha_{mn}} \tag{1}$$

where A_m is the input signal at port m and α_{mn} is the phase difference between input ports. In this work, a Butler matrix with four inputs and four outputs has been designed. The output phase difference is $\pm 45^\circ$ and $\pm 135^\circ$, and crossovers are implemented with two hybrid couplers in cascade.

The hybrid coupler is the key design part since the rest of the elements are based on it. By applying Barlett's [21, 22] theorem to two stages hybrid coupler resolution the following equations are drawn:

$$\begin{aligned} \left(\frac{Z_{02}}{Z_0}\right)^2 &= \frac{2Z_{01}Z_{03}}{Z_0^2 + Z_{01}^2} \\ \left(\frac{Z_{01}}{Z_0}c_0 - 1\right) &= 1 - c_0^2 \end{aligned} \tag{2}$$

where c_0^2 is the power ratio between ports 2 and 3. In this case, the design condition is $c_0^2 = \frac{1}{2}$. There are three missing values (Z_{01}, Z_{02} and Z_{03}) and only two equations. Therefore a degree of freedom exists. In this case, the periodic solution ($Z_{02} = Z_0$) is selected.

As it can be seen in Figure 3, a plain response is obtained for transmission parameters (S_{21} and $S_{31} \approx -3\,\text{dB}$). Besides, the reflection coefficient and the isolation are adequate (S_{11} and $S_{41} < -17\,\text{dB}$). The phase difference between the outputs is $90 \pm 5^\circ$ along the whole

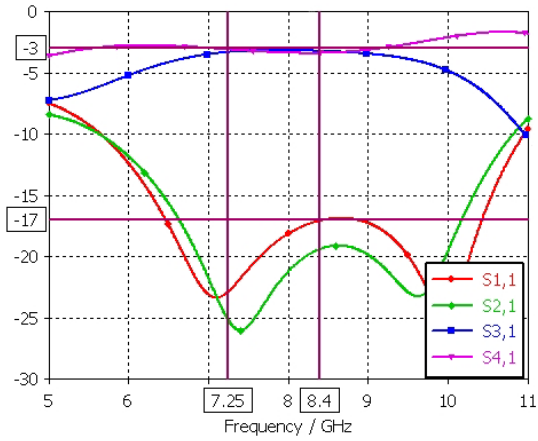

Figure 3. S parameters of hybrid coupler in two stages.

bandwidth [23]. The prototype of the Butler network can be seen in Figure 6.

2.3. Complete System

The phase difference obtained with the Butler network ($\pm 45°$ and $\pm 135°$) is used to feed the antenna array. The desired steering angles 45°, 75°, 105° and 135° are obtained through the array expression:

$$\theta|_{\psi=0} = \arccos\left(\frac{-\alpha}{kd}\right) \tag{3}$$

The complete antenna is an array, with the capability of electronic steering in elevation ($\pm 45°$) with a passive network, and a 360° azimuth steering with a motorized junction. Regarding the frequency range chosen, although 7.25–8.4 GHz range is commonly used nowadays in satellite communications, this design can work properly in a frequency range from 7–9 GHz (25%).

3. CONSTRUCTION AND MEASUREMENTS

An antenna prototype has been built to measure the radiation patterns and verify the antenna performances.

3.1. Array

First of all, Figure 4(b) shows the bottom part of the construction of the 16 elements array. In this figure, it can be seen the uniform

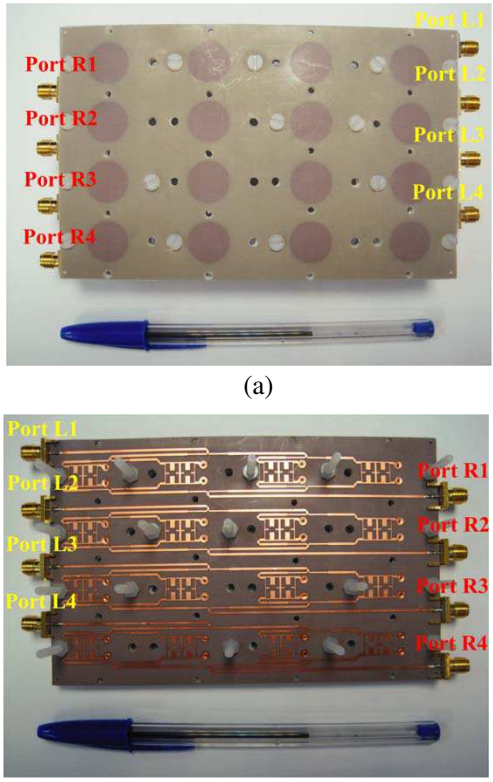

Figure 4. 4×4 array prototype [24]. (a) Top. (b) Bottom.

feeding distribution network, the miniaturized hybrid couplers and the connectors, which will be connected to the steering network. If the Butler network is connected to left side ports, the antenna radiation will be LHCP and vice versa. The rest of the ports will be loaded with $50\,\Omega$ loads.

Figure 5 presents eight input ports of the sixteen elements array. The continuous line show the left side ports, the dashed line represents the right side ports and the marked line corresponds to the isolation between two ports together. The isolation is proper enough with a value under 15 dB for the whole band ($S_{LR} < -15\,\text{dB}$) and the reflection coefficient for all the ports is under $-10\,\text{dB}$ ($S_{ii} < -10\,\text{dB}$).

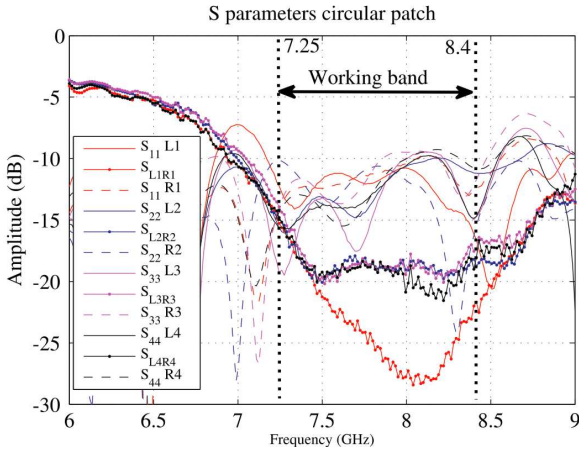

Figure 5. S parameters measurements of 4×4 array prototype (8 ports).

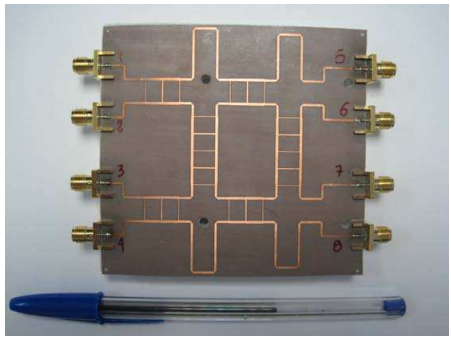

Figure 6. Butler network prototype.

3.2. Steering Network

In the second place, Figure 6 shows the Butler network prototype, the hybrid coupler simulated in 2.2, phase shifters and crossovers. Crossovers are compound of two hybrid couplers in cascade. This passive circuit allows to cross different lines in the substrate without using multilayered structures with good isolation. Therefore, the signal that enters through port 1 goes out through port 4, meanwhile the signal in port 3 it is canceled because its components have a π phase difference. Likewise, signal in port 2 goes to port 3 and it is canceled in port 4. Phase shifters are based in transmission lines, which introduce

a phase shift of 45°, as well as they compensate the electrical length of crossovers. This circuit is electrically large and it can not be included in the same layer of the distribution network. For that reason, it is built in a different printed circuit board. Nevertheless, in this way, it can be used for both TX and RX.

In Figure 7, the S parameter amplitudes of the Butler network are presented. Theoretically, the output power distribution is -6 dB in each port. However, due to the fabrication process, reflection coefficients, losses and isolation level of the circuits the output distribution is -6.5 ± 2 dB (continuous line). The final isolation between ports is better than 12 dB (dashed line).

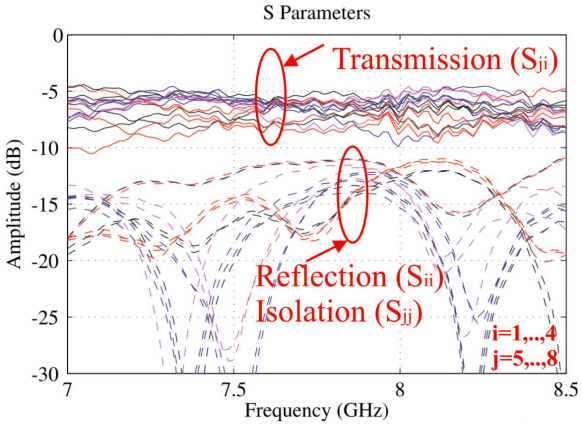

Figure 7. S parameters in amplitude of Butler network.

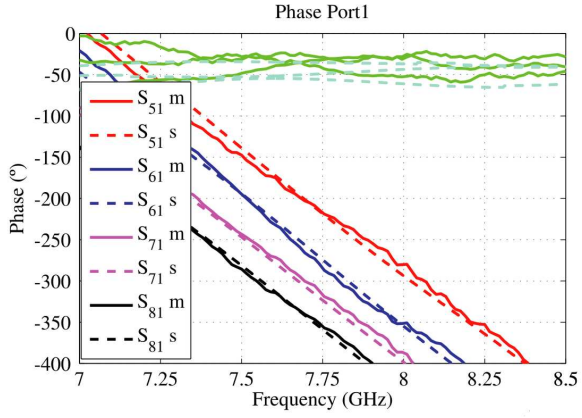

Figure 8. S parameters in phase of Butler network (Port 1).

In Figures 8 and 9 the output phase is shown. It can be seen that the simulations (dashed line) are in good agreement with the measurements (continuous line). When input signal enters in port 1 the phase difference between the outputs is $-45\pm5°$, shown in Figure 8. Figure 9 shows the phase difference between the outputs $+135 \pm 5°$ when the input signal enters in port 2, and the other inputs are loaded with $50\,\Omega$. Similar results are obtained for ports 3 and 4, with the difference that for port 3 the phase difference is $-135\pm5°$ and $+45\pm5°$ for port 4.

3.3. Measurement Setup

Figure 10 shows the 16 elements array connected to the Butler network through low loss cables. The antenna has been measured at the facilities of Technical University of Madrid (UPM).

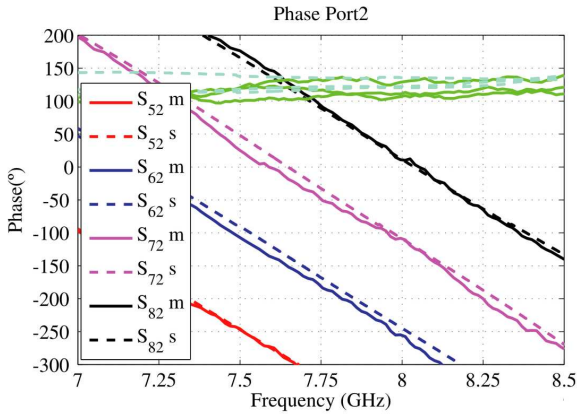

Figure 9. S parameters in phase of Butler network (Port 2).

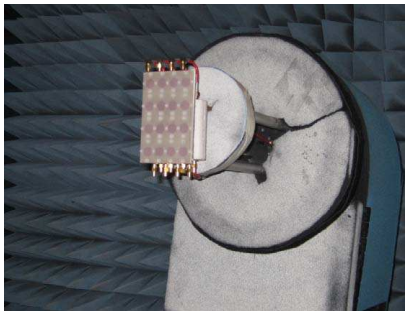

Figure 10. Measurement setup in the anechoic chamber.

In Figures 11 and 12 the radiation patterns at the center frequency of each band (7.5 GHz and 8.15 GHz) for every steering angle are shown. The steering angles $-45°$, $-15°$, $+15°$ and $+45°$ correspond to phase difference feed $\alpha = 135°$ (purple), $\alpha = 45°$ (red), $\alpha = -45°$ (black) and $\alpha = -135°$ (blue) respectively, as it was calculated in Section 2.3. The continuous line presents the measured data, while the dashed one shows simulated data, which are in good agreement. Cross-polar component is represented in dotted line.

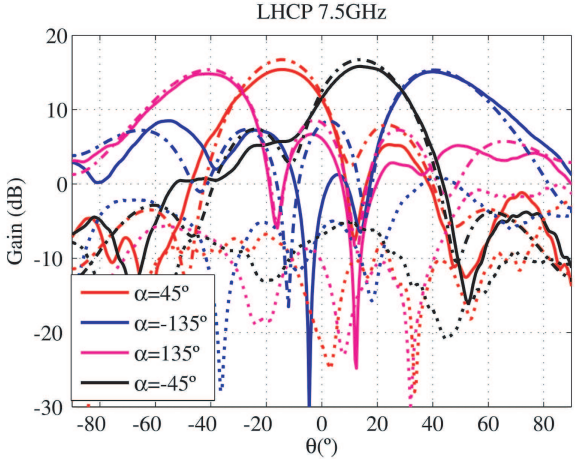

Figure 11. Steering radiation pattern (LHCP 7.5 GHz).

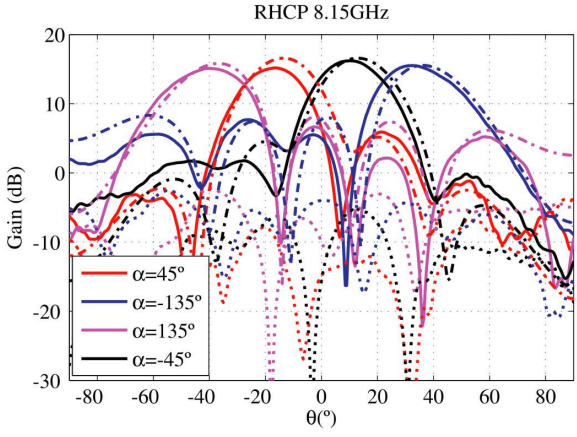

Figure 12. Steering radiation pattern (RHCP 8.15 GHz).

It can be seen in both figures (Figures 11 and 12) a gain reduction in the main beam far from the broadside direction. This is reasonable due to the main beam widening. The level differences between measurements (marked line) and simulations (dashed line) are because of the fact that loss tangent in the dielectric substrate, cables and connectors were not accurately taken into account.

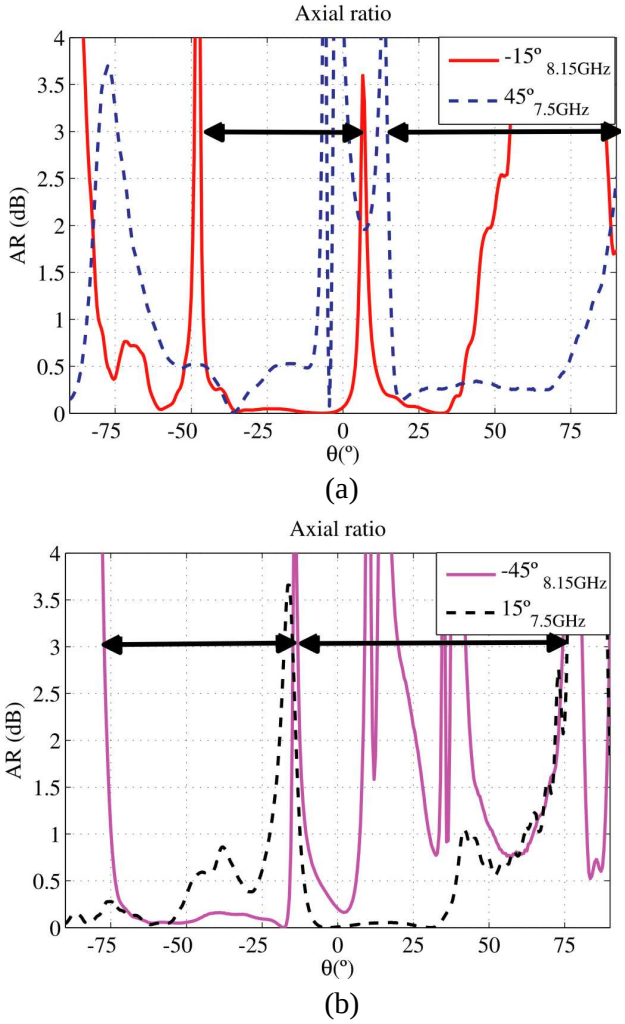

Figure 13. Axial ratio of the different steering beams for θ angles. (a) $-15°$ and $+45°$. (b) $+15°$ and $-45°$.

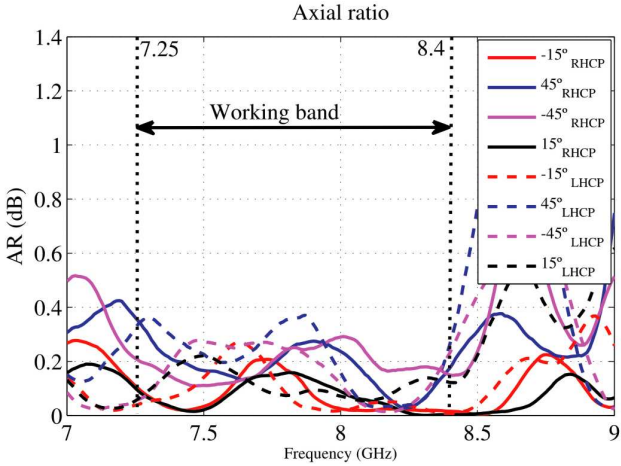

Figure 14. Axial ratio of the different steering beams for different frequencies.

Figure 13 presents the axial ratio of the main beams ($-45°$, $-15°$, $15°$ and $45°$) for the different frequencies and different polarizations ($\text{LHCP}_{7.5\,\text{GHz}}$ and $\text{RHCP}_{8.15\,\text{GHz}}$). It can be seen in this Figure 13 that axial ratio for each pointing beam in an angular range of $\pm 25°$ is under -3 dB.

The CP/XP is larger than 20 dB in the main beam for the different steering directions. In Figure 14, the variation of the axial ratio at the steering direction versus frequency is presented. As expected, the values of circular polarization purity for the main beam are under 1 dB. This result is far better than axial ratio in [25].

4. CONCLUSIONS

In this work a wide band printed antenna with electronic steering capability has been presented. The different parts: feeding distribution network, hybrid coupler and Butler network have been developed in order to get wide band, two circular polarizations (RHCP and LHCP) and an adequate isolation between transmission and reception bands. As it has been conveniently mentioned, the demanding requirements of the antenna system joined to the space constraints turn the design of both, the complete system and each constituting elements, a challenging one, with particular solutions to be added in the design process. This design is validated with the construction and measurements of the antenna prototype.

ACKNOWLEDGMENT

The simulations contained in this work have been carried out using CST Microwave Studio Suite 2011 under a cooperation agreement between Computer Simulation Technology (CST) and Universidad Politécnica de Madrid. We kindly thank the company NELTEC S.A. for giving samples of the substrates, in which the prototypes were built. This work is been supported by an UPM grant CH/003/2011, the project CG10-UPM/TIC-5805 and the CROCANTE project with reference TEC2008-06736-C03-01.

REFERENCES

1. Salas Natera, M. A., A. García Aguilar, J. Mora Cuevas, J. M. Fernández, P. Padilla de la Torre, J. García-Gasco Trujillo, R. Martínez Rodríguez Osorio, M. Sierra Pérez, L. de Haro Ariet, and M. Sierra Castañer, "Satellite communications," *New Antenna Array Architectures for Satellite Communications*, Chapter 7, 167–194, InTech Open Access Publisher, Jul. 2011.
2. Balanis, C. A., *Antenna Theory Analysis and Design*, John Wiley & Sons, 2005.
3. Vogt, G., "An electronic method for steering the beam and polarization of HF antennas," *IEEE Transactions on Antennas and Propagation*, Vol. 10, No. 2, 193–200, Mar. 1962.
4. Topalli, K., O. A. Civi, S. Demir, S. Koc, and T. Akin, "A monolithic phased array using 3-bit distributed RF MEMS phase shifters," *IEEE Transactions on Microwave Theory and Techniques*, Vol. 56, No. 2, 270–277, Feb. 2008.
5. Vaccaro, S., D. Llorens del Rio, J. Padilla, and R. Baggen, "Low cost Ku-band electronic steerable array antenna for mobile satellite communications," *Proceedings of the 5th European Conference on Antennas and Propagation (EUCAP)*, 2362–2366, Apr. 2011.
6. Peng, H.-L., W.-Y. Yin, J.-F. Mao, D. Huo, X. Hang, and L. Zhou, "A compact dual-polarized broadband antenna with hybrid beam-forming capabilities," *Progress In Electromagnetics Research*, Vol. 118, 253–271, 2011.
7. Blass, J., "Multi-directional antenna — new approach top stacked beams," *IRE International Convention Record*, 48–50, 1960.
8. Butler, J. and R. Lowe, "Beam-forming matrix simplifies design of electronically scanned antennas," *Electronic Design*, Vol. 9, 170–173, Apr. 1961.

9. Rao, K. S., G. A. Morin, M. Q. Tang, S. Richard, and K. K. Chan, "Development of a 45 GHz multiple-beam antenna for military satellite communications," *IEEE Transactions on Antennas and Propagation*, Vol. 43, No. 10, Oct. 1995.
10. Liang, G., W. Gong, H. Liu, and J. Yu, "Development of 61-channel digital beamforming (DBF) transmitter array for mobile satellite communication," *Progress In Electromagnetics Research*, Vol. 97, 177–195, 2009.
11. Walter, C. H., *Traveling Wave Antennas*, McGraw-Hill, 1965.
12. Hines, J. N., V. H. Rumsey, and C. H. Walter, "Traveling-wave slot antennas," *Proceedings of the IRE*, Vol. 41, No. 11, 1624–1631, Nov. 1953.
13. Wang, A.-N. and W.-X. Zhang, "Design and optimization of broadband circularly polarized wide-slot antenna," *Journal of Electromagnetic Waves and Applications*, Vol. 23, No. 16, 2229–2236, 2009.
14. Chen, D. and C. H. Cheng, "A novel compact ultra-wideband (UWB) wide slot antenna with via holes," *Progress In Electromagnetics Research*, Vol. 94, 343–349, 2009.
15. García-Aguilar, A., J. M. Inclán-Alonso, L. Vigil-Herrero, J. M. Fernández-González, and M. Sierra-Pérez, "Printed antenna for satellite communications," *2010 IEEE International Symposium on Phased Array Systems and Technology*, 529–535, Boston, EE.UU., Oct. 2010.
16. Liao, W.-J., S.-H. Chang, Y.-C. Chu, and W.-S. Jhong, "A beam scanning phase array for UHF RFID readers with circularly polarized patches," *Journal of Electromagnetic Waves and Applications*, Vol. 24, No. 17–18, 2383–2395, 2010.
17. Islam, M. T., M. N. Shakib, and N. Misran, "Design analysis of high gain wideband L-probe fed microstrip patch antenna," *Progress In Electromagnetics Research*, Vol. 95, 397–407, 2009.
18. Tang, C. W. and M. G. Chen, "Synthesizing microstrip branch-line couplers with predetermined compact size and bandwidth," *IEEE Transactions on Microwave Theory and Techniques*, Vol. 55, No. 9, 1926–1934, Sep. 2007.
19. Garg, R., I. Bahl, and A. Ittipiboon, *Microstrip Antennas Design Handbook*, Artech House, 2001.
20. James, J. R. and P. S. Hall, *Handbook of Microstrip Antennas*, IEEE Waves Series, Peter Peregrinus Ltd., 1989.
21. Pozar, D. M. and D. H. Schaubert, *Microstrip Antennas: The Analysis and Design of Microstrip Antennas and Arrays*, IEEE

Press, 1995.

22. Matthaei, G. and L. Young, *Microwave Filters, Impedance-Matching Networks, and Coupling Structures*, Artech House Publishers, 2000.
23. Expósito-Domínguez, G., P. Padilla-Torre, J. M. Fernández-González, and M. Sierra-Castañer, "Matriz de Butler de Banda Ancha en Banda X para antenas reconfigurables," *XXV URSI Spain*, Bilbao, Spain, Sep. 2010.
24. Expósito-Domínguez, G., P. Padilla-Torre, J. M. Fernández-González, and M. Sierra-Castañer, "Electronic steering antenna onboard for satellite communications in X band," *5th European Conference on Antennas and Propagation (EuCAP 2011)*, 2120–2123, Rome, Italy, Apr. 2011.
25. Du, S., Q.-X. Chu, and W. Liao, "Dual-band Circularly polarized stacked square microstrip antenna with small frequency ratio," *Journal of Electromagnetic Waves and Applications*, Vol. 24, No. 11–12, 1599–1608, 2010.